Notch signaling licenses allergic airway inflammation by promoting Th2 cell lymph node egress

Irma Tindemans[1], Anne van Schoonhoven[1,2], Alex KleinJan[1], Marjolein J.W. de Bruijn[1], Melanie Lukkes[1], Menno van Nimwegen[1], Anouk van den Branden[1], Ingrid M. Bergen[1], Odilia B.J. Corneth[1], Wilfred F.J. van IJcken[3], Ralph Stadhouders[1,2]*# and Rudi W. Hendriks[1]*#

(1) Department of Pulmonary Medicine, Erasmus MC Rotterdam, the Netherlands

(2) Department of Cell Biology, Erasmus MC Rotterdam, the Netherlands

(3) Center for Biomics, Erasmus MC Rotterdam, the Netherlands

* Shared senior authorship

Corresponding author

Correspondence to:

Ralph Stadhouders & Rudi W. Hendriks

Department of Pulmonary Medicine, Erasmus MC Rotterdam

PO Box 2040, 3000 CA Rotterdam, the Netherlands

e-mail: r.stadhouders@erasmusmc.nl & r.hendriks@erasmusmc.nl

phone: ++31-10-7043700

Supplemental data:

- 6 Supplemental Figures

- 2 Supplemental Tables
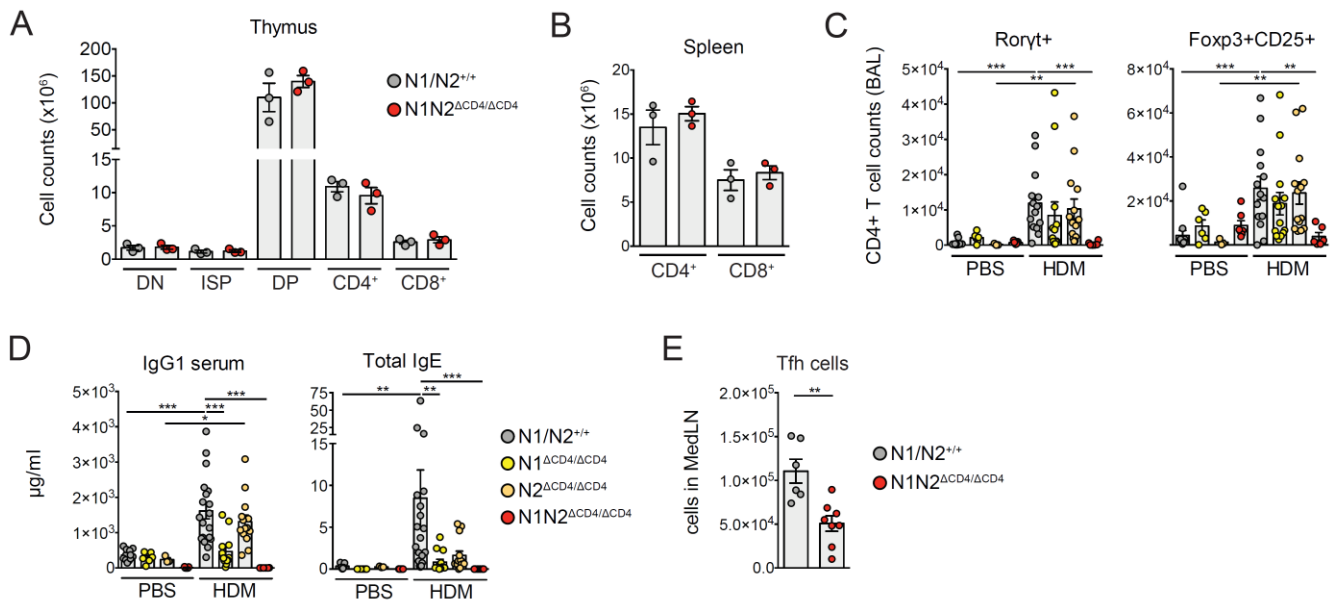
Supplemental Figure 1. Notch signaling in CD4$^+$ T cells does not affect T cell development, but is required for AAI induction. (**A**) Numbers of total cells in each thymocyte subpopulation in WT and N1N2$^{\Delta CD4/\Delta CD4}$ mice, as determined by flow cytometry; DN, CD3$^-$CD4$^-$CD8$^-$ double negative cells; ISP, CD3$^-$CD4$^-$CD8$^+$ immature single positive cells; DP, CD3$^+$CD4$^+$ double positive cells, CD4$^+$, CD4$^+$CD8$^-$ CD3$^+$ T cells; CD8$^+$, CD4$^-$CD8$^+$ CD3$^+$ T cells. (**B**) Quantification of the total numbers of CD4$^+$ and CD8$^+$ T cells in the spleens of WT and N1N2$^{\Delta CD4/\Delta CD4}$ mice. (**C**) Quantification of Rorγt$^+$CD4$^+$ Th17 cells and Foxp3$^+$CD25$^+$ regulatory T cells in the BAL fluid of mice subjected to an acute HDM-driven AAI protocol (see Figure 1A). (**D**) Concentrations of total IgG1 and IgE in the serum of mice subjected to an acute HDM-driven AAI protocol, as determined by ELISA. (**E**) Number of PD1$^+$CXCR5$^+$ follicular T helper (Tfh) cells in the MedLN of WT and N1N2$^{\Delta CD4/\Delta CD4}$ mice subjected to an acute HDM-driven AAI protocol. Data are shown as individual values, together with the mean ± SEM from 3 (panels A-B) or 6-8 mice per group (panels C-D). *p<0.05, **p<0.01, ***p<0.001, Kruskal-Wallis test (panel A-D) or Mann-Whitney U-test (panel E).
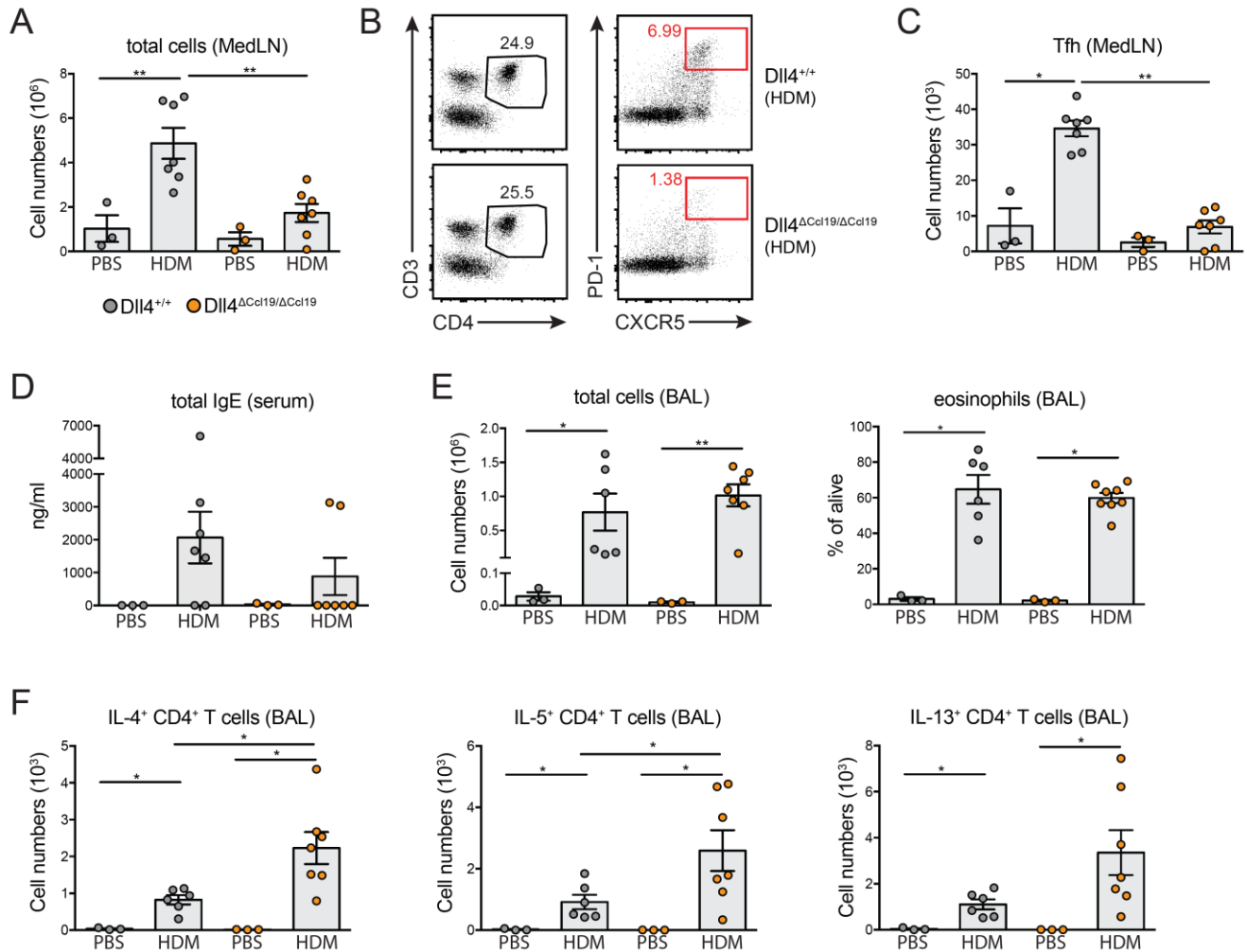
Supplemental Figure 2. DLL4 expression on CCL19$^+$ MedLN fibroblastic reticular cells is required for Tfh formation and IgE induction, but not for eosinophilia in an acute HDM-driven AAI model. (**A**) Total numbers of MedLN cells in Dll4$^{\Delta Ccl19/\Delta Ccl19}$ and Dll4$^{+/+}$ WT mice in acute HDM-driven AAI, according to the protocol depicted in Figure 1A. (**B-C**) Flow cytometry gating (B) and quantification (C) of the numbers of CD3$^+$CD4$^+$PD-1$^+$CXCR5$^+$ follicular T helper (Tfh) cells in MedLN of PBS or HDM-sensitized Dll4$^{+/+}$ and Dll4$^{\Delta Ccl19/\Delta Ccl19}$ mice. (**D**) Serum IgE levels as determined by ELISA of the indicated genotypes. (**E**) Numbers of total cells and FSC^{int}SSC^{high}Siglec-F$^+$ eosinophils in BAL fluid of PBS or HDM-sensitized Dll4$^{+/+}$ and Dll4$^{\Delta Ccl19/\Delta Ccl19}$ mice. (**F**) Numbers of CD4$^+$ T cells positive for the indicated cytokines by intracellular flow cytometry in BAL fluid of PBS or HDM-sensitized Dll4$^{+/+}$ and Dll4$^{\Delta Ccl19/\Delta Ccl19}$ mice. Data are shown as individual values, together with the mean ± SEM from 3-7 mice per group. *p<0.05, **p<0.01; Kruskal-Wallis test.

A — CD3+ T cells (Lung)

B — CD69+ Trm (Lung)

N1N2+/+
N1N2ΔCD4/ΔCD4

C — IL-4+ CD4+ T cells (Lung); IL-5+ CD4+ T cells (Lung); IL-13+ CD4+ T cells (Lung)

D — IL-4+ CD4+ T cells (BAL); IL-5+ CD4+ T cells (BAL); IL-13+ CD4+ T cells (BAL)

E — Total IgG1; Total IgE

F — GC B cells; Tfh cells

G — GC B cells; Tfh cells

N1/N2+/+
N1N2ΔCD4/ΔCD4

4
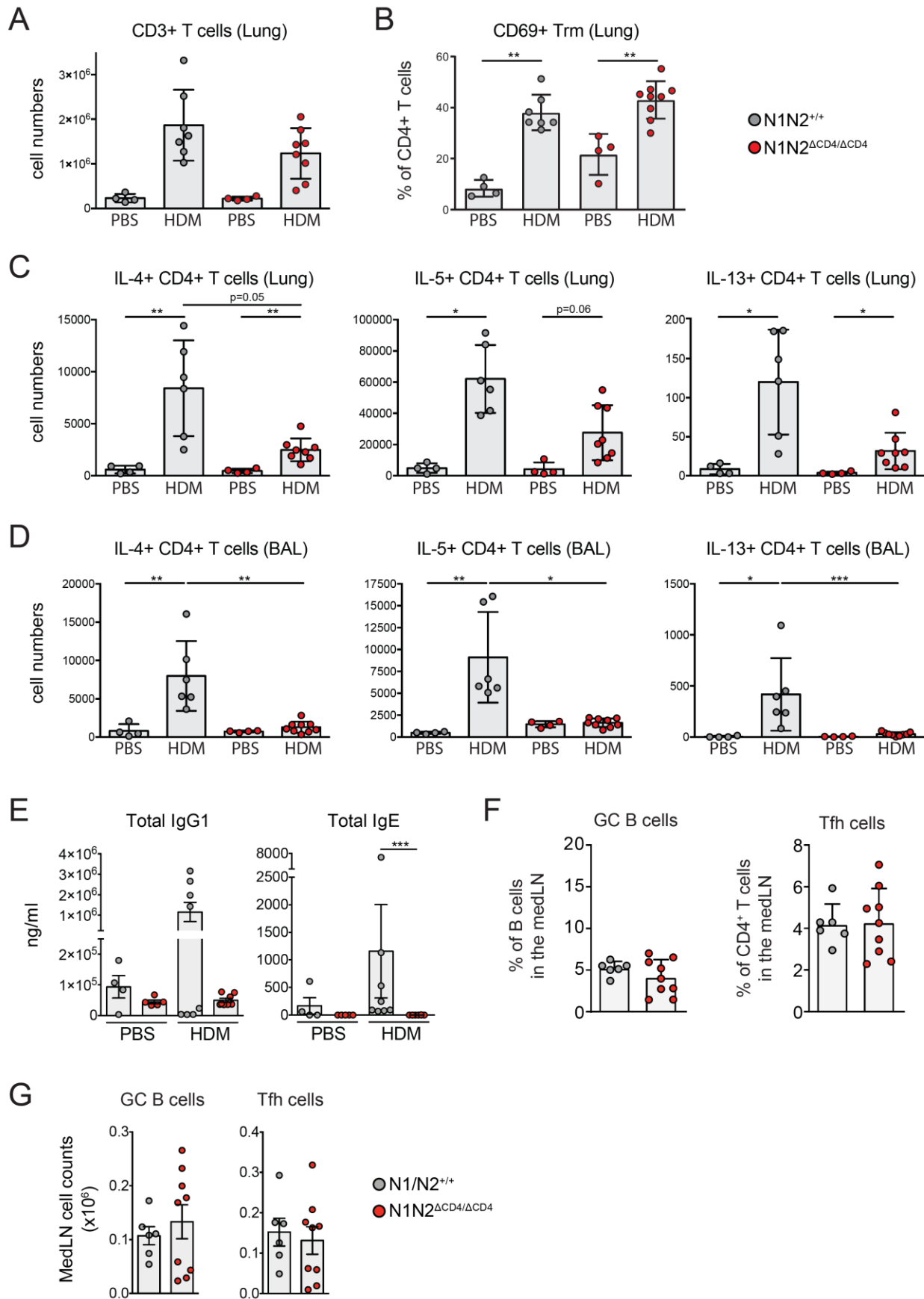
Supplemental Figure 3. Cytokine production by lung CD4$^+$ T cells and IgE induction in HDM-driven AAI is dependent on Notch signaling. (**A-B**) Numbers of total CD3$^+$ T cells (A) and the proportions of CD69$^+$ resident memory T (Trm) cells (B) in the lungs of PBS or HDM-sensitized mice of WT and N1N2$^{\Delta CD4/\Delta CD4}$ mice subjected to chronic HDM-driven AAI, according to the protocol depicted in **Figure 2A**. (**C-D**) Numbers of CD4$^+$ T cells positive for the indicated cytokines by intracellular flow cytometry in lung (C) or BAL fluid (D) of PBS or HDM-sensitized mice of the indicated genotype. (**E**) Total IgG1 and IgE levels as determined by ELISA in serum of PBS or HDM-sensitized WT and N1N2$^{\Delta CD4/\Delta CD4}$ mice subjected to chronic HDM-driven AAI, according to the protocol depicted in Figure 2A. (**F-G**) Numbers (panel F) and proportions (panel G) of GL7$^+$CD95$^+$IgD$^-$ GC B cells (*left*) and follicular T helper (Tfh) cells in the MedLN of mice of the indicated genotype. Data are shown as individual values, together with the mean ± SEM of 4-9 mice per group. *p<0.05, **p<0.01; Kruskal-Wallis test (panel A-E) or Mann-Whitney U-test (panel F-G).
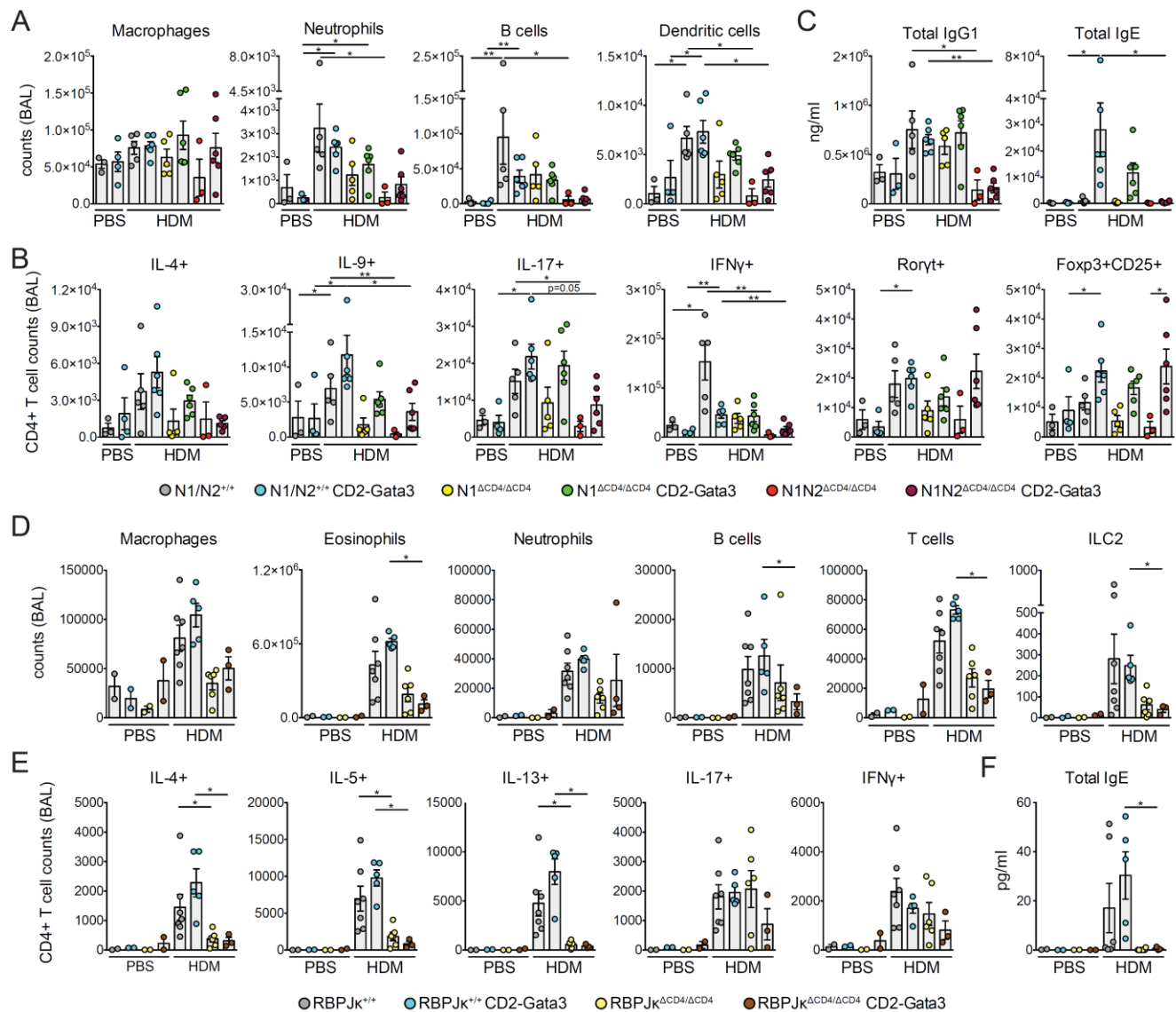
Supplemental Figure 4. Limited rescue of AAI in Notch-deficient mice by enforced Gata3 expression. (**A**) Numbers of macrophages (FSC^{high}SSC^{high+}CD11c$^+$Siglec-F$^+$ autofluorescent cells), neutrophils (Ly-6G$^+$ cells), B cells (CD19$^+$ cells) and DCs (CD11c$^+$MHCII^{hi} cells) in BAL fluid of PBS or HDM-sensitized mice challenged with HDM as indicated in Figure 1A. (**B**) Absolute numbers of cytokine-expressing CD3$^+$CD4$^+$ T cells, Rorγt$^+$CD4$^+$ Th17 cells and Foxp3$^+$CD25$^+$ regulatory T cells in the BAL fluid of the indicated PBS or HDM-sensitized mice. (**C**) Concentrations of total IgG1 and IgE in the serum of mice subjected to an acute HDM-driven AAI protocol, as determined by ELISA. (**D**) Numbers FSC^{high}SSC^{high+}CD11c$^+$Siglec-F$^+$ autofluorescent macrophages, FSC^{int}SSC^{high}Siglec-F$^+$ eosinophils, Ly-6G$^+$ neutrophils, CD19$^+$ B cells, CD3$^+$ T cells and Lineage$^-$IL-7R$^+$T1ST2$^+$ type 2 innate lymphoid cells (ILC2) in BAL fluid from four groups of PBS- or HDM-sensitized WT or RBPJκ-deficient mice. (**E**)

Absolute numbers of cytokine-expressing CD3$^+$CD4$^+$ T cells in the BAL fluid of PBS or HDM-sensitized mice. (**F**) Concentrations of total IgE in the serum of indicated mice subjected to an acute HDM-driven AAI protocol, as determined by ELISA. Data are shown as individual values, together with the mean values ± SEM of 3-7 mice per group and are representative of 3 independent experiments. *p<0.05, **p<0.01; Kruskal-Wallis test.
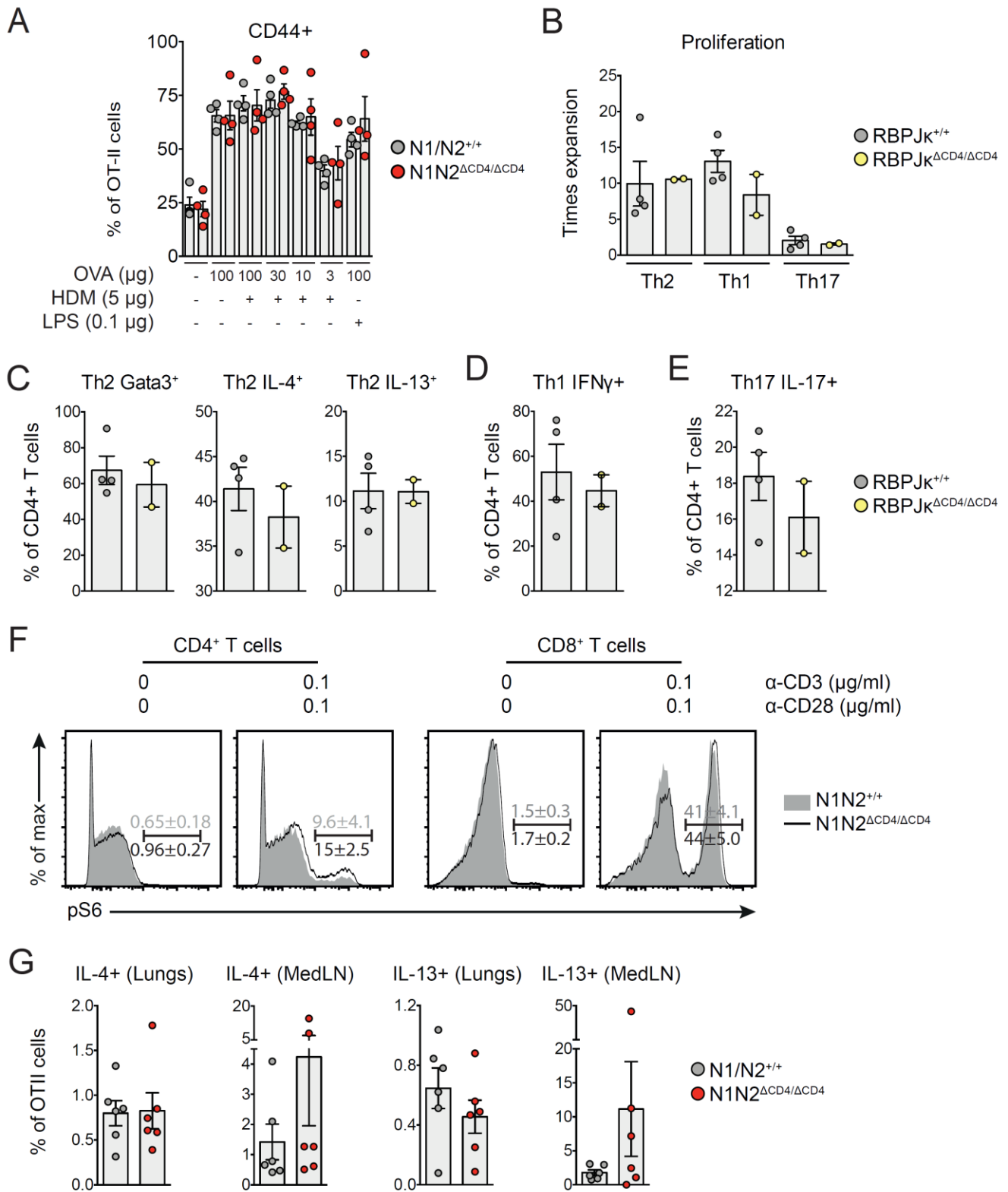
Supplemental Figure 5. Notch signaling is not required for in vitro proliferation and differentiation of CD4+ T cells. (**A**) Proportions of splenic WT and N1N2$^{\Delta CD4/\Delta CD4}$ CD4+ T cells

expressing surface CD44 upon in vitro activation with the indicated stimuli. (**B**) In vitro expansion of purified splenic WT and RBPJκ $^{\Delta CD4/\Delta CD4}$ CD4$^+$ T cells activated with anti-CD3 and anti-CD28 antibodies and cultured under Th1, Th2 and Th17-polarizing conditions. Total numbers of cells at the start of the culture were set to 1. (**C**) Proportions of Gata3 and Th2 cytokine positive CD4$^+$ T cells within in vitro polarized Th2 cultures from WT and RBPJκ $^{\Delta CD4/\Delta CD4}$ mice, as determined by flow cytometry. (**D**) Proportions of IFNγ CD4$^+$ T cells from in vitro polarized Th1 cultures from WT and RBPJκ $^{\Delta CD4/\Delta CD4}$ mice. (**E**) Proportions of IL-17$^+$ CD4$^+$ T cells from in vitro polarized Th17 cultures from WT and RBPJκ $^{\Delta CD4/\Delta CD4}$ mice. (**F**) Total spleen cells from WT and N1N2$^{\Delta CD4/\Delta CD4}$ mice were stimulated with the indicated concentrations of α-CD3 and α-CD28 for 3 hours, after which phosphorylation of the ribosomal protein S6 in CD4$^+$ and CD8$^+$ T cells was measured using flow cytometry. (**G**) Percentages of IL-4$^+$ and IL-13$^+$ OTII CD4$^+$ T cells in the lung and MedLN of mice that received in vitro Th2-polarized OTII CD4$^+$ T cells that were either WT of N1N2$^{\Delta CD4/\Delta CD4}$, as determined by flow cytometry. Data are shown as individual values, together with the mean values ± SEM of 2-6 mice per group and are representative of two independent experiments.
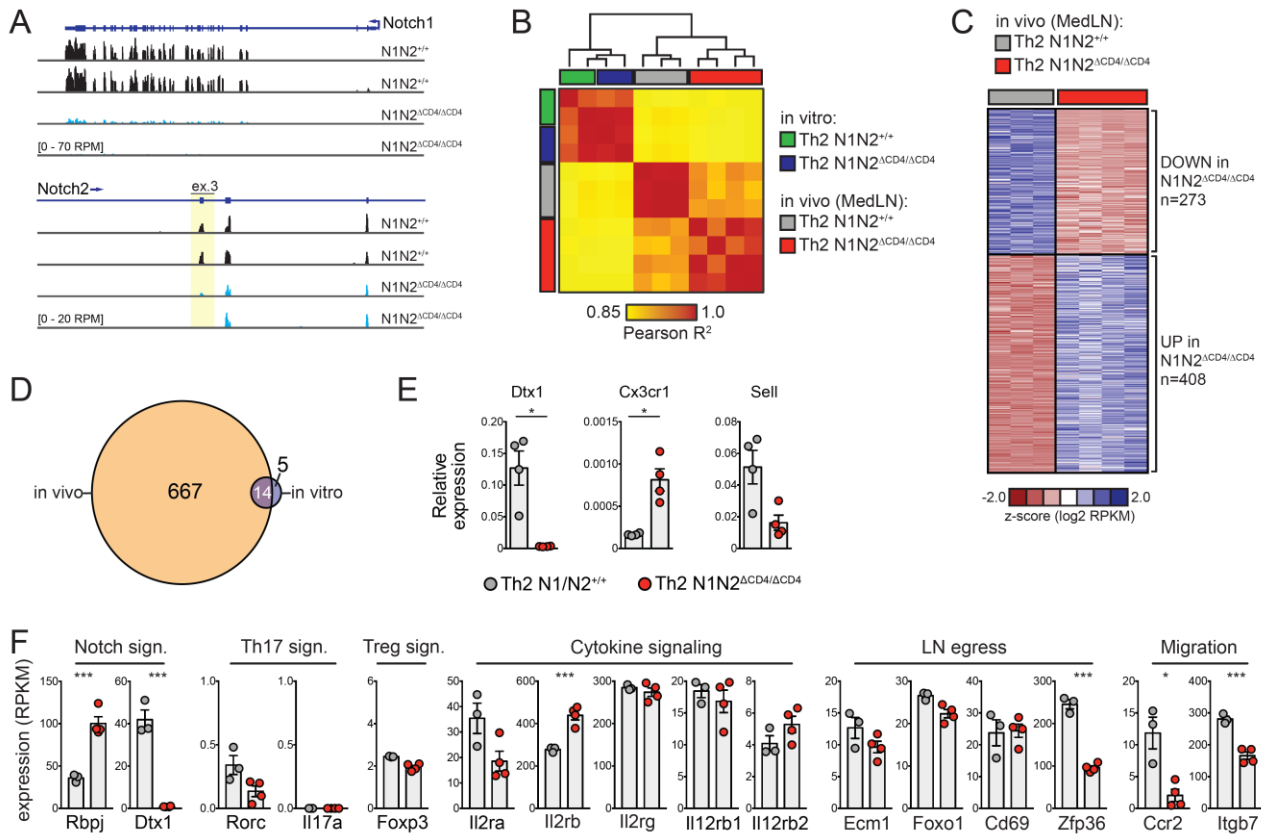
Supplemental Figure 6. Transcriptional deregulation in Th2 cells due to Notch1/2 deficiency.
(**A**) IGV genome browser screenshots of RNA-Seq signals from WT (N1N2$^{+/+}$) and Notch-deficient (N1N2$^{\Delta CD4/\Delta CD4}$) OTII Th2 cells after in vitro polarization across the *Notch1* gene (top) and the *Notch2* floxed critical exon 3 (bottom). (**B**) Unsupervised hierarchical clustering of genome-wide RNA-Seq expression values from WT (N1N2$^{+/+}$) and Notch-deficient (N1N2$^{\Delta CD4/\Delta CD4}$) OTII Th2 cells after in vitro polarization or 5 days after in vivo transfer and OVA/HDM-treatment. Heatmap depicts correlation strength (Pearson R^2) amongst the datasets. (**C**) Heatmap showing differentially expressed (DE) genes between WT and Notch-deficient Th2 cells from MedLN. (**D**) Venn diagram indicating the overlap in the sets of DE genes detected 'in vitro' (WT versus Notch-deficient Th2 cells directly after polarization in vitro) or 'in vivo' (WT versus Notch-deficient Th2 cells from the MedLN after in vivo transfer and OVA/HDM treatment). (**E**) Quantitative PCR validations of DE genes detected by RNA-Seq comparing WT and Notch-deficient Th2 cells from the MedLN. (**F**) Expression levels of selected genes; data are shown as individual values, together with the mean values ± SEM of 3-4 biological replicates. *p<0.05, **p<0.01, ***p<0.001, using a Mann-Whitney U-test (panel E) or adjusted DESeq2 p-values (panel F).

Supplemental Table 1. Antibodies used in this study

Target	Conjugate	Company	Clone	Application
B220	APC	BD Biosciences	RA3-6B2	Flowcytometry
B220	PE	eBioscience	RA3-6B2	Flowcytometry
CCR4	BV421	Biolegend	SA214G2	Flowcytometry
CCR8	PE-Cy7	Biolegend	2G12	Flowcytometry
CD3	APC-ef780	eBioscience	17A2	Flowcytometry
CD3	BV421	BD Biosciences	145-2C11	Flowcytometry
CD3	PE	eBioscience	145-2C11	Flowcytometry
CD3	PE-CF594	BD biosciences	145-2C11	Flowcytometry
CD4	AF700	eBioscience	GK1.5	Flowcytometry
CD4	APC-H7	BD Biosciences	GK1,5	Flowcytometry
CD4	BV605	BD Biosciences	RM4-5	Flowcytometry
CD4	BV711	BD Biosciences	RM4-5	Flowcytometry
CD4	FITC	eBioscience	RM4-5	Flowcytometry
CD4	PE	eBioscience	RM4-5	Flowcytometry
CD4	PerCP-Cy5.5	eBioscience	RM4-5	Flowcytometry
CD5	PE	eBioscience	53-7.3	Flowcytometry
CD8a	FITC	eBioscience	Ly-2	Flowcytometry
CD8	PE	eBioscience	Ly-2	Flowcytometry
CD8a	PE-Cy7	eBioscience	53-6.7	Flowcytometry
CD11b	APC	eBioscience	M1/70	Flowcytometry
CD11b	PE	eBioscience	M1/70	Flowcytometry
CD11c	BV786	BD Biosciences	HL3	Flowcytometry
CD11c	PE	eBioscience	N418	Flowcytometry
CD19	AF700	eBioscience	eBio1D3	Flowcytometry
CD19	APC-ef780	eBioscience	1D3	Flowcytometry
CD19	PE	BD Biosciences	1D3	Flowcytometry
CD25	PE-Cy7	eBioscience	PC61.5	Flowcytometry
CD25	PerCP-Cy5.5	eBioscience	PC61.5	Flowcytometry
CD44	APC	BD Biosciences	IM7	Flowcytometry
CD44	APC-Cy7	BD Biosciences	IM7	Flowcytometry
CD44	FITC	eBioscience	IM7	Flowcytometry
CD44	PerCP-Cy5.5	eBioscience	IM7	Flowcytometry
CD62L	APC	eBioscience	MEL-14	Flowcytometry
CD127	e450	eBioscience	A7R34	Flowcytometry
CD127	PE-Cy7	eBioscience	A7R34	Flowcytometry

CXCR4	APC	BD Biosciences	2B11	Flowcytometry
FcεRIα	PE	eBioscience	MAR-1	Flowcytometry
Foxp3	AF488	eBioscience	FJK-16s	Flowcytometry
Foxp3	PE-Cy7	eBioscience	FJK-16s	Flowcytometry
Gata3	ef660	eBioscience	TWAJ-14	Flowcytometry
IFN-γ	BV650	BD Biosciences	XMG1.2	Flowcytometry
IFN-γ	e450	eBioscience	XMG1.2	Flowcytometry
IFN-γ	PE-Cy7	eBioscience	XMG1.2	Flowcytometry
IL-4	BV711	BD Biosciences	11B11	Flowcytometry
IL-4	PE	BD Biosciences	11B11	Flowcytometry
IL-5	APC	BD Biosciences	TRFK-5	Flowcytometry
IL-5	PE	BD Biosciences	TRFK-5	Flowcytometry
IL-5	Biotin	BD Biosciences	TRFK4	Flowcytometry
IL-9	PE	BD Biosciences	D9302C12	Flowcytometry
IL-10	AF488	eBioscience	JES5-16E3	Flowcytometry
IL-10	PerCP-Cy5.5	eBioscience	JES5-16E3	Flowcytometry
IL-13	ef450	eBioscience	eBio13A	Flowcytometry
IL-13	ef660	eBioscience	eBio13A	Flowcytometry
IL-17A	AF700	BD Biosciences	TC11-18H10.1	Flowcytometry
Live/Dead	Amcyan	Invitrogen		Flowcytometry
Ly-6A/Ly-6E	BV786	BD Biosciences	D7	Flowcytometry
Ly-6G	PE-Cy7	BD Biosciences	1A8	Flowcytometry
Ly-6C/Ly-6G	APC-ef780	eBioscience	RB6-8C5	Flowcytometry
Ly-6C/Ly-6G	PE	eBioscience	RB6-8C5	Flowcytometry
MHC class II	AF700	eBioscience	M5/114.15.3	Flowcytometry
NK1.1	Horizon 450	BD Biosciences	PK136	Flowcytometry
NK1.1	PE	eBioscience	PK136	Flowcytometry
Rorγt	PE	BD Biosciences	Q31-378	Flowcytometry
Siglec-F	PE	BD Biosciences	E50-2440	Flowcytometry
Streptavidin	APC-ef780	eBioscience		Flowcytometry
Streptavidin	BV711	BD Biosciences		Flowcytometry
Streptavidin	BV785	BD Biosciences		Flowcytometry
Streptavidin	PE-Cy7	eBioscience		Flowcytometry
T1/ST2 (IL-33R)	Biotin	mdbiosciences, Zürich, Swiss	DJ8	Flowcytometry
T1/ST2 (IL-33R)	FITC	mdbiosciences	DJ8	Flowcytometry

T-bet	BV421	BD Biosciences	O4-46	Flowcytometry
TCR vα2	APC-Cy7	BD Biosciences	B20.1	Flowcytometry
TCR vα2	Biotin	eBioscience	B20.1	Flowcytometry
TCR vβ5.1, 5.2	Biotin	BD Biosciences	MR9-4	Flowcytometry
TCR vβ5.1, 5.2	BV785	BD Biosciences	MR9-4	Flowcytometry
TER-119	PE	eBioscience	TER119	Flowcytometry
CXCR3	BV711	BD Biosciences	CXCR3-173	Flowcytometry
CXCR5	Biotin	BD Biosciences	2G8	Flowcytometry
PD-1	BV421	BD Biosciences	J43	Flowcytometry
CD69	PE	eBioscience	H1.2F3	Flowcytometry
CD103	ef450	eBioscience	2E7	Flowcytometry
gp38	PE	Biolegend	eBio8.1.1	Flowcytometry
CD31	FITC	eBioscience	390	Flowcytometry
GL7	FITC	BD Biosciences	GL7	Flowcytometry
CD95	PE	BD Biosciences	Jo2	Flowcytometry
IgD	BV711	BD Biosciences	11-26c.2a	Flowcytometry
CD3	APC-ef780	eBioscience	17A2	Histology
IgM	FITC	BD Biosciences	II/41	Histology
GL7	FITC	BD Biosciences	GL7	Histology
IgD	PE	eBioscience	11-26c	Histology
Goat-anti-rat IgG	AP	CiteAb	polyclonal	Histology
Goat-anti-FITC IgG	PO	Rockland	polyclonal	Histology
Goat-anti-FITC IgG	AP	Rockland	polyclonal	Histology
Goat-anti-PE IgG	PO	Rockland	polyclonal	Histology

Supplemental Table 2. RNA-Seq data analysis (see accompanying .xlsx file)